Analyzing the Birth and Propagation of Two Distinct Prions, [*PSI*+] and [Het-s]y, in Yeast

Vidhu Mathur,* Vibha Taneja,*† Yidi Sun,‡ and Susan W. Liebman*

*Department of Biological Sciences, University of Illinois, Chicago, IL 60607; and ‡Department of Molecular and Cell Biology, University of California, Berkeley, CA 94720

Various proteins, like the infectious yeast prions and the noninfectious human Huntingtin protein (with expanded polyQ), depend on a Gln or Asn (QN)-rich region for amyloid formation. Other prions, e.g., mammalian PrP and the [Het-s] prion of *Podospora anserina*, although still able to form infectious amyloid aggregates, do not have QN-rich regions. Furthermore, [Het-s] and yeast prions appear to differ dramatically in their amyloid conformation. Despite these differences, a fusion of the Het-s prion domain to GFP (Het-sPrD-GFP) can propagate in yeast as a prion called [Het-s]y. We analyzed the properties of two divergent prions in yeast: [Het-s]y and the native yeast prion [*PSI*+] (prion form of translational termination factor Sup35). Curiously, the induced appearance and transmission of [*PSI*+] and [Het-s]y aggregates is remarkably similar. Overexpression of tagged prion protein (Sup35-GFP or Het-sPrD-GFP) in nonprion cells gives rise to peripheral, and later internal, ring/mesh-like aggregates. The cells with these ring-like aggregates give rise to daughters with one (perivacuolar) or two (perivacuolar and juxtanuclear) dot-like aggregates per cell. These line, ring, mesh, and dot aggregates are not really the transmissible prion species and should only be regarded as phenotypic markers of the presence of the prions. Both [*PSI*+] and [Het-s]y first appear in daughters as numerous tiny dot-like aggregates, and both require the endocytic protein, Sla2, for ring formation, but not propagation.

INTRODUCTION

The mammalian prion is an infectious form of the PrP protein that causes transmissible, neurodegenerative diseases (Prusiner, 1998), also known as transmissible spongiform encephalopathies (TSEs). TSEs are characterized by the conversion of the normal, cellular form of the mammalian prion protein, PrP^C, into a misfolded, insoluble, amyloid-like prion form, PrP^Sc. The conversion from normal to prion form is accompanied by a structural change in PrP^C from an α-helical– to a β-sheet–rich conformation (Pan *et al.*, 1993), which facilitates the formation of amyloid-like fibrils.

Prions in fungi also form infectious amyloid-like aggregates. The known prions in *Saccharomyces cerevisiae*, namely [*PSI*+], [*PIN*+], [URE3], [*SWI*+], [*OCT*+], [*MCA1*], and [*MOT3*+] (Wickner, 1994; Wickner *et al.*, 1995; Sondheimer and Lindquist, 2000; Derkatch *et al.*, 2001; Du *et al.*, 2008; Alberti *et al.*, 2009; Nemecek *et al.*, 2009; Patel *et al.*, 2009) and the [Het-s] prion of the filamentous fungus *Podospora anserina* (Coustou *et al.*, 1997), are all inherited cytoplasmically. Many of them have been shown to appear spontaneously, be protease resistant, and form insoluble amyloid aggregates in vivo and in vitro (Wickner, 1994; Coustou *et al.*, 1997; King *et al.*, 1997; Derkatch *et al.*, 2001; Brachmann *et al.*, 2005; Patel and Liebman, 2007; Alberti *et al.*, 2009).

[*PSI*+] is the prion form of the yeast translation termination factor Sup35. The Sup35 protein consists of three do-

mains: the QN-rich N-terminal prion domain (amino acids 1-123), the charged middle M-domain (amino acids 124-254), and the functional C-domain (amino acids 255-685). Although the C-domain is necessary and sufficient for translation termination and viability, the N-domain of Sup35 is necessary and sufficient for [*PSI*+] prion formation and propagation in vivo (Derkatch *et al.*, 1996) and amyloid-like fiber formation in vitro (King *et al.*, 1997; Glover *et al.*, 1997; Serio *et al.*, 2000). Inactivation of Sup35, e.g., when in the form of prion aggregates, causes readthrough of premature stop codons (nonsense suppression).

The overexpression of full-length Sup35 or the Sup35NM domains enhances [*PSI*+] formation in the presence of another prion [*PIN*+] (Derkatch *et al.*, 1996, 1997, 2000), which is the prion form of the Rnq1 protein (Sondheimer and Lindquist, 2000; Derkatch *et al.*, 2001). The function of Rnq1 is unknown, but its prion form enhances de novo [*PSI*+] formation. The overexpression of Sup35NM fused to green fluorescent protein (GFP) in [psi−] [*PIN*+] cells gives rise to ring-, line-, and dot-like [*PSI*+] aggregates (Zhou *et al.*, 2001). The ring-like aggregates are either peripheral, along the cell membrane, or internal, surrounding the vacuole (Ganusova *et al.*, 2006). When Sup35-GFP expression is at the Sup35 endogenous level, [*PSI*+] propagates as numerous tiny dots (Satpute-Krishnan and Serio, 2005).

[*PSI*+] and [*PIN*+] can occur in multiple, stable conformations known as prion variants. Although [*PSI*+] variants can be weak or strong, defined by the relative efficiency of the associated nonsense suppression (Derkatch *et al.*, 1996), [*PIN*+] exists as low, medium, high, and very high variants that are characterized by the efficiency with which they promote [*PSI*+] induction (Bradley *et al.*, 2002; Bradley and Liebman, 2003). Overexpression of Sup35NM-GFP in either strong or weak [*PSI*+] variants usually gives rise to cells with single large fluorescent foci. Overexpression of Rnq1-

Table 1. Yeast strains used in this study

Strains	Description	Reference/Source
74D-694	*MATa ade1-14 ura3-52 leu2-3,112 trp1-289 his3-200*	Derkatch *et al.* (1996)
L1749	74D-694 [*psi⁻*] multidot high [*PIN⁺*]	Derkatch *et al.* (1996)
L1943	74D-694[*psi⁻*] single dot low [*PIN⁺*]	Derkatch *et al.* (1996)
L2910	74D-694[*psi⁻*][*pin⁻*]	Derkatch *et al.* (1996)
L1749 *act1-1*	74D-694 [*psi⁻*][*PIN⁺*] *act1R177A*	This study
L2903	*MATα* 74D-694 *SUP35::SUP35-GFP* [*psi⁻*]high[*PIN⁺*]	This study
L2245	*MATα ura2 leu2* strong [*PSI⁺*][*pin⁻*]	Bradley *et al.* (2002)
L2285	*MATα ura2 leu2* [*psi⁻*][*pin⁻*]	Bradley *et al.* (2002)
L2785	*MATα ade2-1 lys1-1 his3-11 leu1 kar1-1 URA3::KanMX4 canᴿ multidot high* [*PIN⁺*]	This study
SY84	74D-694 *SUP35::SUP35-GFP* [*psi⁻*][*pin⁻*]	Satpute-Krishnan and Serio (2005)
GF822	74D-694 *SUP35::SUP35-GFP* [*psi⁻*][*PIN⁺*] *GST-DsRed (UGA)*	Satpute-Krishnan and Serio (2005)
GT88	74D-694 [*psi⁻*][*PIN⁺*] *sla1::HIS3*	Ganusova *et al.* (2006)
GF683	*MATa his3Δ1 leu2Δ0 met15Δ0 ura3Δ0 end3::KanMX*	Yeast deletion library; Invitrogen
DDY130	*MATa his3-Δ200 leu2-3, 112 ura3-52 lys2-801*	Sun *et al.* (2005)
DDY2740	*MATa his3-Δ200 leu2-3,112 ura3-52 lys2-801 sla2::cgLEU2* [*psi⁻*][*pin⁻*]	Sun *et al.* (2005)
DDY1194	*MATa/MATα sla2Δ768-968::URA3/sla2Δ768-968::URA3 leu2/leu2 lys2/lys2 ura3/ura3 his3/his3 ade2/+* [*psi⁻*][*pin⁻*]	Yang *et al.* (1999)
DDY1195	*MATα/MATα sla2Δ501-968::URA3/sla2Δ501-968::URA3 leu2/leu2 lys2/lys2 ura3/ura3 his3/his3 ade2/+* [*psi⁻*][*pin⁻*]	Yang *et al.* (1999)
DDY426	*MATa/MATα ura3-52/ura3-52 his3Δ200/his3Δ200 leu2-3,112/leu2-3,112 lys2-801oc/lys2-801oc ade2-101am/+*	Yang *et al.* (1999)

GFP in [*PIN⁺*] variants generally gives rise to cells with a single large fluorescent dot (for low, medium, and very high [*PIN⁺*]s) or multiple smaller dots (for high [*PIN⁺*]).

A common feature of [*PSI⁺*], [*PIN⁺*], and other yeast prions is the presence of Gln or Asn (QN)-rich regions (DePace *et al.,* 1998; Osherovich *et al.,* 2004; Ross *et al.,* 2005) resembling polyQ proteins like huntingtin, which is involved in Huntington's disease. However, unlike the known yeast prions, but like the mammalian prion PrP�Sᶜ, the [Het-s] prion of *P. anserina* lacks QN-rich regions. The HET-s protein, composed of 289 amino acids, functions in heterokaryon incompatibility only in its prion form (Coustou *et al.,* 1997). The C-terminus (amino acids 218–289) of Het-s is sufficient for prion formation and is thus considered to be the prion domain (Balguerie *et al.,* 2003). Evidence suggests that the QN-rich prion domain structures of Sup35, Rnq1, and Ure2 are parallel in-register β-sheet (Shewmaker *et al.,* 2006, 2008, 2009; Baxa *et al.,* 2007; Wickner *et al.,* 2008a,b) or possibly cross β-helix for Sup35NM (Kishimoto *et al.,* 2004; Krishnan and Lindquist, 2005; Nelson *et al.,* 2005). In contrast, the HET-s prion domain appears to form a β-solenoid structure (Ritter *et al.,* 2005; Sen *et al.,* 2007; Wasmer *et al.,* 2008).

Despite these compositional and structural differences, the prion domain of HET-s fused to GFP (Het-sPrD-GFP) propagates as a prion, [Het-s]ᵧ, in yeast (Taneja *et al.,* 2007). Similar to [*PSI⁺*] (Zhou *et al.,* 2001), overexpression of Het-sPrD-GFP gives rise to ring-like aggregates that later propagate as two dot aggregates in each cell (Taneja *et al.,* 2007). Although [*PIN⁺*] enhances [Het-s]ᵧ ring formation twofold, it is not required for [Het-s]ᵧ appearance.

Mutations in endocytic proteins inhibit de novo [*PSI⁺*] and polyQ aggregation and enhance the toxicity associated with [*PSI⁺*] and polyQ (Bailleul *et al.,* 1999; Ganusova *et al.,* 2006; Meriin *et al.,* 2007). Although *sla2Δ* essentially prevents, and *sla1Δ*, *end3Δ*, and *act1-1* reduce, de novo [*PSI⁺*] formation upon over expression of *SUP35NM-GFP*, the spe-

cific role of these endocytic proteins in prion formation is unknown.

Here, we present an in-depth analysis of the appearance of prion rings and dots during the birth and propagation of the native QN-rich prion, [*PSI⁺*], and a foreign non-QN-rich prion, [Het-s]ᵧ. We also analyze the effects of endocytic mutations on this process.

MATERIALS AND METHODS

Strains, Plasmids, and Growth Conditions

The yeast strains used in this study are listed in Table 1. L1749, L1943, and L2910 are derivatives of 74D-694 (Derkatch *et al.,* 1996). SY84 (74D-694 *SUP35::SUP35-GFP* [*psi⁻*] [*pin⁻*]) was a gift from Tricia Serio (Brown University) (Satpute-Krishnan and Serio, 2005). L2903 was made by cytoducing multidot, high [*PIN⁺*] from L2785 into SY84. L1749 *act1-155* was made in L1749 using the plasmid pKWF46-R177A as described (Ganusova *et al.,* 2006).

Plasmids used in this study are listed in Table 2. p1834 (*Tet0-SLA2*) was constructed by putting the full *SLA2* ORF under the *Tet0* box repressor in pCM184 (Gari *et al.,* 1997).

Table 2. Plasmids used in this study

Plasmids	Description	Reference
p1393	P_{GAL1}-*Het-sPrD-GFP, TRP1*	Taneja *et al.* (2007)
p1525	P_{GAL1}-*Het-sPrD (T266P)-GFP, TRP1*	Taneja *et al.* (2007)
p1470	P_{GAL1}-*Het-sPrD-CFP, URA3*	This study
p1066	P_{CUP1}*SUP35NM-GFP, URA3*	Zhou *et al.* (2001)
pDD353	P_{SLA2}-*SLA2, HIS3*	Yang *et al.* (1999)
pDD362	*sla2Δ33-750, HIS3*	Yang *et al.* (1999)
pDD364	*sla2Δ33-501, HIS3*	Yang *et al.* (1999)
pDD367	*sla2Δ33-359, HIS3*	Yang *et al.* (1999)
pDD369	*sla2Δ33-359, 576ˢᵗᵒᵖ HIS3*	Yang *et al.* (1999)
pDD371	*sla2Δ360-575, HIS3*	Yang *et al.* (1999)
pCM184	Vector with *Tet0* operator, *TRP1*	Gari *et al.* (1997)
p1834	*Tet0-SLA2, TRP1*	This study

All yeast strains were grown in standard media (Sherman *et al.*, 1986) at 30°C, except the *sla2Δ* strains that were grown at 25°C. Yeast transformations used the lithium acetate method (Gietz and Woods, 2002). For induction of [Het-s]y rings, transformants were grown in liquid 2% raffinose synthetic medium (SR) overnight, then transferred to liquid SR + 2% galactose (2% Gal) medium for ~24 h for ring formation, and then subcultured into SR + 0.05% galactose plates (0.05% Gal) for dot formation. For induction of [PSI+] rings, p1066 transformants were grown in selective medium supplemented with 50–150 μM CuSO$_4$ for ~24 h. Micromanipulation of single cells was done on a 2% Noble agar patch that was then transferred to an agar plate of desired media.

To test propagation of [Het-s]y dots in the absence of Sla2, plasmids with *Het-sPrD-CFP* (*URA3*; p1470) and *SLA2* (*HIS3*; pDD353) were cotransformed into *sla2Δ* cells, and 90% [Het-s]y dot cultures were obtained by growing cells on 2% Gal to induce rings. Ring cells were then micromanipulated and grown on 0.05% Gal-Ura-His plates. The *SLA2* plasmid was then lost by growing cells on 0.05% Gal-Ura+His. As a control, cultures were grown on 0.05% Gal-Ura-His to keep both plasmids. His− and His+ colonies were respectively replica plated three times consecutively on 0.05% Gal-Ura or 0.05% Gal-Ura-His, and the number of cells with [Het-s]y dots was counted after each transfer.

Fluorescence Microscopy

The [Het-s]y induction frequency was determined as the fraction of cells with fluorescent rings in 2% Gal cultures grown overnight (determined with a Zeiss Axioskop 2; Thornwood, NY). FM4-64 staining was as described (Vida and Emr, 1995). Briefly, cultures with [Het-s]y rings were washed and incubated with 8 μM FM4-64 (Molecular Probes, Eugene, OR) in liquid complex dextrose (YPD) medium for 15 min. Cells were then washed, incubated in YPD for 0, 10, 20, 30, and 60 min, and observed for vacuolar staining at each time point. For nuclear staining, cells were permeabilized with 10% formaldehyde for 2 h and then with 70% ethanol for 30 min at room temperature. The cells were next washed twice with water and an equal amount of DAPI in mounting media (Vector Laboratories, Burlingame, CA) was mixed with the cell suspension after which cells were immediately viewed. The colocalization images were collected as Z-stacks and subjected to 3D deconvolution on a Zeiss Axiovert 200M equipped with a digital camera.

The transition of a cell with a ring to a microcolony of cells with dots was observed as described previously (Mathur *et al.*, 2009). Briefly, single cells with [Het-s]y or [PSI+] rings were micromanipulated onto a 2% Noble agar patch that was grown overnight on 0.05% Gal-Trp and synthetic dextrose (e.g., SD-Ura) plates, respectively. The agar patch was then transferred to a clean glass slide, a coverslip was placed on it, and the cells were examined with fluorescence microscopy. The agar patch, with the coverslip in place, was then returned to plates with respective medium to allow colony growth. The growing colony was then observed similarly every 6–8 h.

Biochemical Analysis of Yeast Cell Lysates

Crude cell extracts were prepared by vortexing cells in 750 μl of lysis buffer (50 mM Tris/HCl, pH 7.5, 50 mM KCl, 10 mM MgCl$_2$, and 5% [wt/vol] glycerol, 1:50 diluted protease inhibitor cocktail [Sigma, St. Louis, MO], and 5 mM PMSF) with 0.5 mm glass beads (Biospec, Bartlesville, OK) at high speed, three times for 1 min, with cooling on ice for 1 min between each vortexing. Lysates were cleared of cell debris by centrifuging them two times at 600 × *g* for 1 min.

For protein analysis, ~50 μg of crude lysate heated (95°C) in 2% SDS sample buffer (25 mM Tris, 200 mM glycine, 5% glycerol, and 0.025% bromophenol blue) with 2% β-mercaptoethanol for 10 min were resolved on 10% polyacrylamide gels and transferred to a polyvinylidene difluoride (PVDF) membrane (Bio-Rad, Richmond, CA). The membranes were probed with the desired antibody. When required, the membrane was stripped of the first antibody, by incubating twice with stripping buffer (100 mM β-mercaptoethanol, 2% SDS, 62.5 mM Tris-Cl, pH 6.8) at 70°C for 30 min, washed three times with washing buffer (1× TBS, 0.1% Tween 20) for 5 min, and then probed with the appropriate antibody.

For coimmunocapture, 0.05–0.5 mg/ml total protein was incubated with or without anti-GFP antibody for 2 h and then magnetic protein G beads (Miltenyi biotec, Auburn, CA) for 30 min. The mixture was passed through magnetic separation columns (Miltenyi biotec), washed with washing buffers, and eluted using heated (95°C) 1× sample buffer with 2% SDS (Bagriantsev *et al.*, 2008). The eluates were run on 10% polyacrylamide gels (Bio-Rad), transferred to PVDF membrane, and probed for specific proteins.

Anti-GFP antibody was from Roche Applied Science (Indianapolis, IN). Anti-Pgk1 was from Invitrogen (Carlsbad, CA). Anti-Sla2 antibodies were as described (Yang *et al.*, 1999).

RESULTS

Appearance and Propagation of [PSI+] Aggregates

To investigate the conversion of rings to dots, cells with rings were micromanipulated, and aggregate appearance was viewed in newly formed buds at several time points. [PSI+] cells, in which genomic *SUP35* is replaced with functional *SUP35-GFP*, have been described to propagate [PSI+]

as numerous, tiny, moving dots, whereas isogenic [psi−] cells show diffuse fluorescence (Satpute-Krishnan and Serio, 2005). Genomic *SUP35NM-GFP* in [psi−] [PIN+] cells formed ring-like aggregates after 16–18 h when Sup35NM-GFP was overexpressed from the *CUP1* promoter. Cells with such rings were micromanipulated to, and grown on, medium lacking additional Cu^{2+}, which turned down the expression of *SUP35NM-GFP* (about eightfold; Supplementary Figure 1) while allowing the endogenous *SUP35-GFP* to be expressed. From the micromanipulated cells with ring or line aggregates, 15 (62 tested) cells with rings and four (18 tested) with lines (examples shown in Figure 1A) grew into colonies. In each case, rings or lines remained in the mother cells and daughters contained multiple, tiny dots indicative of [PSI+] (Figure 1B). The daughters divided further to give rise to a [PSI+] colony with cells having numerous, tiny dots. We observed one or two bigger dots in ~1% of the daughter cells in the microcolonies (not shown) in addition to multi-tiny dots. This is probably due to P$_{CUP1}$ leakiness that allows some Sup35NM-GFP synthesis. Peripheral rings in the mothers shrank inward to surround the vacuole and form an internal ring, while the lines condensed to form one big dot that appeared different from the occasional big dots in daughters. The big dot in the mothers appeared denser and bigger than the dots in daughters, which were brighter and smaller, like punctae. Interestingly, in one micromanipulated cell, we saw that the line aggregate grew to become a peripheral ring along the cell membrane, suggesting that rings are derived from line-like aggregates (Supplementary Figure 2).

Appearance and Propagation of [Het-s]y Aggregates

The yeast system developed for [Het-s]y described by Taneja *et al.* (2007) uses the *GAL1* promoter to overexpress *Het-sPrD-GFP*. [Het-s]y rings are observed in 2% Gal, dots are maintained when ring cells are transferred to 0.05% Gal where the expression of *Het-sPrD-GFP* is reduced 40-fold. Now, we micromanipulated cells induced to form [Het-s]y peripheral rings in 2% Gal and grew them on 0.05% Gal to observe the progression from ring to dot. Similar to our findings for [PSI+] rings, [Het-s]y rings were always retained in the mother cell (in 25 cells observed) and shrank inward to surround the vacuole (Figure 1C and 2A).

In [pin−] cultures, mother cells with [Het-s]y rings gave rise to daughters that initially had no GFP and then diffuse GFP fluorescence. Later these daughters showed numerous, tiny dots (Figure 1C) similar to those seen for [PSI+]. However, unlike [PSI+], these numerous dots later turn into three to four dots and finally to two big dots. During the progression of [Het-s]y rings to dots, the numerous, tiny dots become fewer and fewer in number as the cell ages. Cells with two dots do not have any observable tiny dots.

In [PIN+] cultures, mother cells with [Het-s]y rings gave rise to daughters with no GFP fluorescence, then diffuse GFP fluorescence, and finally two dots as seen in [pin−] cells (Figure 1D and Supplementary Figure 3) without going through a visible multiple tiny dot stage. All daughters retained their dots as they budded off their daughters. [Het-s]y ring-to-dot generation in [PSI+] [pin−] cells mimicked that seen in [psi−] [pin−] cells (Figure 1C), indicating that, unlike [PIN+], the [PSI+] prion does not accelerate [Het-s]y aggregation. Our attempts to see if [Het-s]y could propagate as numerous visible dots like [PSI+], by lowering the expression of Het-sPrD-GFP (using 0.01% Gal), failed. Even at lower expression levels, [Het-s]y propagated as two large dots.

The peripheral rings form along the maximum width of the cells. In many cases, the de novo [Het-s]y aggregates appeared as a mesh of rings along the inner cell membrane
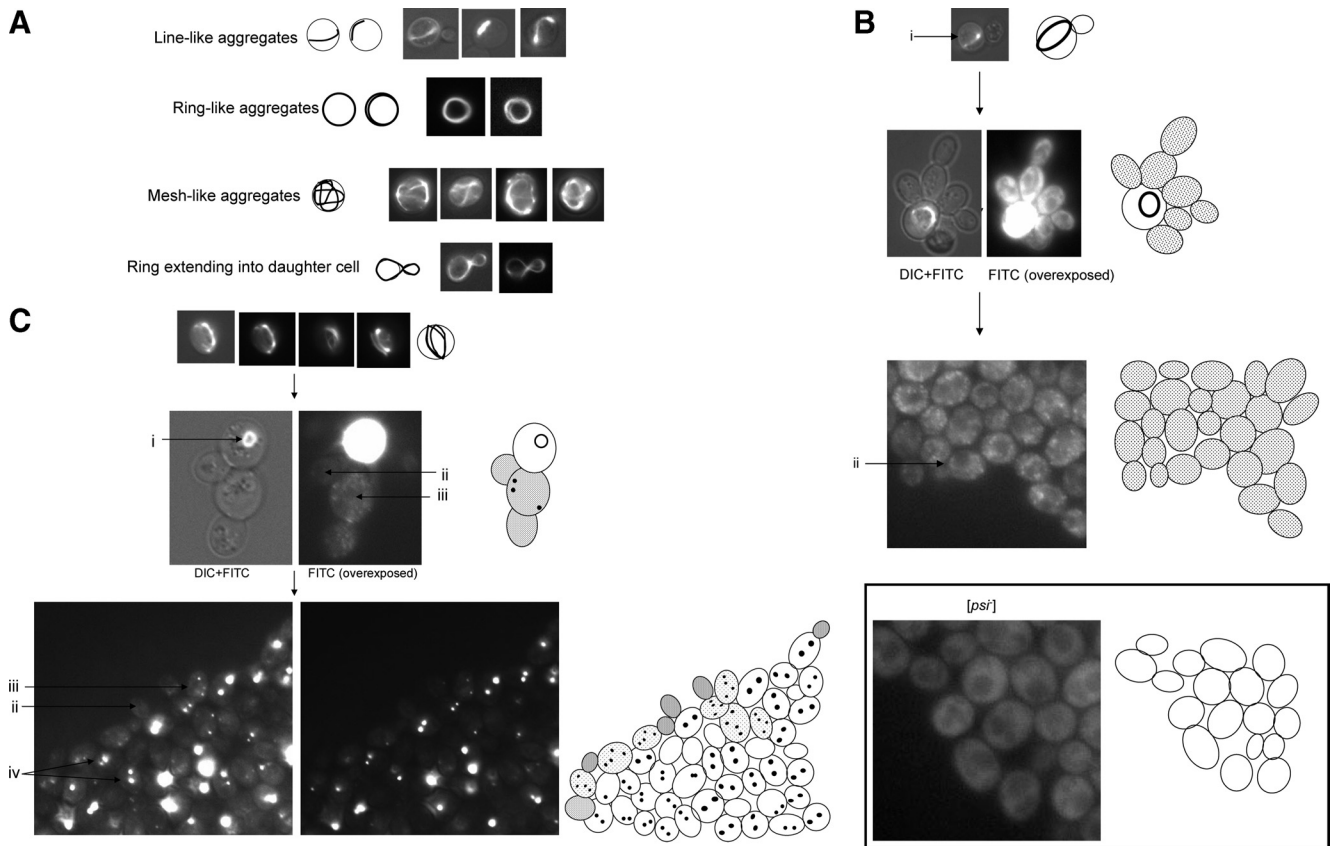
Figure 1. Appearance of prion rings and dots. (A) Types of de novo prion aggregates. [PSI^+] and [Het-s]$_y$ de novo aggregates were induced by overexpressing Sup35NM-GFP or Het-sPrD-GFP in [psi^-] [PIN^+] cells (L1749). Shown here are fluorescent images of cells showing line-like aggregates (confirmed by moving focal plane up and down), ring-like aggregates, mesh-like aggregates, and ring aggregates extending into the daughter cells. The diagram represent 2D view of the cells. (B) [PSI^+] ring-to-dot progression. Sup35NM-GFP was overexpressed (from p1066) in [psi^-] [PIN^+] cells containing endogenous *SUP35-GFP* (L2903) to form rings. Cells with rings (i) were micromanipulated, grown on plates lacking Cu^{2+}, and observed every 6–8 h. Shown is a cell with a ring giving rise to daughters with numerous, with tiny dots characteristic of [PSI^+] (ii). The second panel is a DIC image merged with fluorescence (left) and bright fluorescence image (right) where tiny moving dots, hard to capture with the camera, were clearly seen by eye. The third panel shows a fluorescence image of part of the mature colony showing [PSI^+] cells with numerous tiny dots. The diagrams depict the images seen. [psi^-] cells are shown in the box. (C and D). [Het-s]$_y$ ring-to-dot progression. Het-sPrD-GFP (p1393) was overexpressed in [psi^-] [pin^-] (L2910) (C) or [psi^-] [PIN^+] (L1749) (D) cells. Cells with [Het-s]$_y$ rings and meshes were micromanipulated and observed every 6–10 h. The top panel in C shows different layers of the same cell with a mesh aggregate. The middle panel (left, DIC+FITC) shows the same mother cell later with an internal ring surrounding the vacuole (i). Its daughter cells (right, overexposed fluorescence) first showed numerous tiny dots (ii), which then coalesced revealing two to four bigger dots (iii). Bottom panels show two exposures of a part of the mature colony. Older cells have two dots (iv), whereas the new daughters first have numerous dots and proceed as their mothers. In D, [psi^-] [PIN^+] cells with an [Het-s]$_y$ ring (i) gave rise to daughters that did not show any fluorescence initially and then showed diffuse fluorescence (v; cannot be seen in the picture because the fluorescence images were taken with DIC. Supplementary Figure 3 shows cells with diffuse fluorescence.), and later two dots appeared (iv). Similarly, all daughters again give rise to cells with two dots. Some cells in the figure show only one dot, because the other dot is in another focal plane and could be seen when the focus was moved up and down. (E) Ring-, line-, and dot-containing cells have the [PSI^+] phenotype. Sup35NM-GFP (p1066) was overexpressed in [psi^-] [PIN^+] DsRed(UGA) cells (GF822) and analyzed for red fluorescence. Cells with either rings, lines, or dots show red fluorescence. Control cells with diffuse Sup35NM-GFP did not show red fluorescence.

(Figure 1A). In some cells these rings/mesh aggregates can be clearly visualized by eye to be continuous when examined by slowly moving the focal plane up and down; however, in cells with extensive meshes we cannot be certain of the continuity of the rings/meshes (see Supplemental Movies 1–8). Sometimes, the peripheral ring/mesh appeared to enter the daughter cell, again along the inner membrane of the daughter (Figure 1A). Three of seven such [Het-s]$_y$ mother-daughter pairs that were micromanipulated, continued to divide. The rings in these mothers and daughters continued to shrink inward to surround the vacuole, and each mother and daughter ring cell gave rise to daughters with two dots. Similar aggregates spanning mother and daughter were also occasionally observed for [PSI^+] and such peripheral rings,

internal rings, rings going into the daughters, and one big dot in cells have also been observed with overexpression of full-length, untagged Sup35 via immunofluorescence (Zhou *et al.*, 2001). Thus, the GFP-tagged Sup35NM that we have used in this study mimics full-length Sup35 and is physiologically relevant. Unfortunately, the Het-s antibody did not work when we attempted to use it to similarly visualize untagged Het-sPrD.

To test how the [PSI^+]-associated phenotype of suppression of stop codons was correlated with Sup35NM-GFP ring/line/dot aggregates, we took advantage of the GST-DsRed(UGA) allele, which shows red fluorescence in [PSI^+], but not in [psi^-] cells (Satpute-Krishnan and Serio, 2005). Sup35NM-GFP was overexpressed in [psi^-] [PIN^+] cells
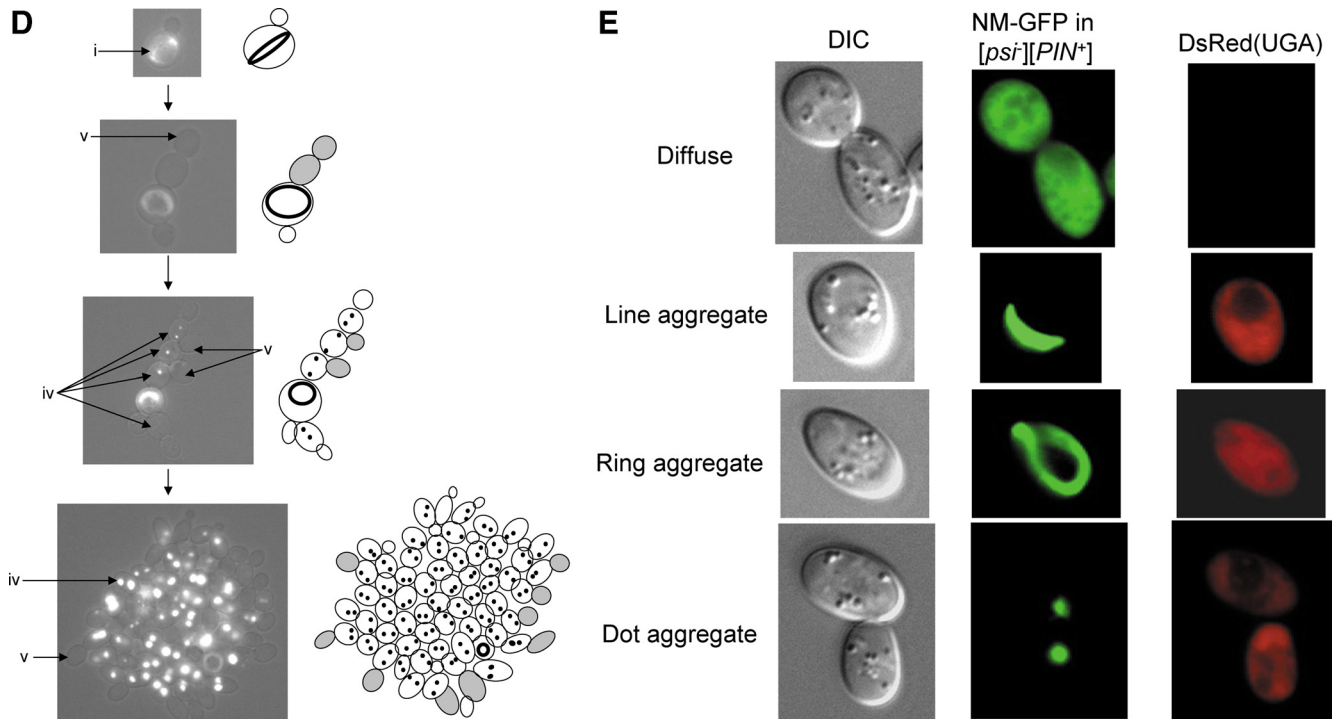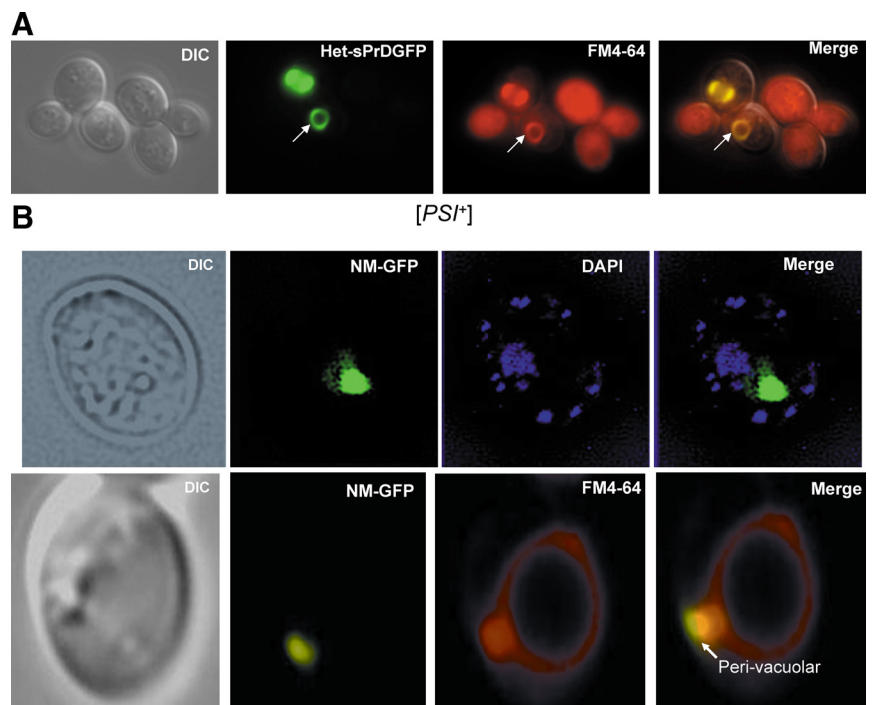
Figure 1. *Continued.*

containing GST-DsRed(UGA). Cells with Sup35NM-GFP rings, lines, and dots, but not control diffuse cells, showed the appearance of red fluorescence, indicating suppression of the UGA stop codon in DsRed (Figure 1E).

[*PSI*⁺], [*PIN*⁺], and [Het-s]ᵧ Dots Localize to Perivacuolar and Juxtanuclear Compartments

A recent study showed that misfolded proteins can accumulate in two distinct quality control compartments in *cim3-1*

yeast mutants that inhibit degradation of ubiquitinated proteins via the proteasomes (Kaganovich *et al.*, 2008). Ubiquitinated proteins were shown to accumulate in a juxtanuclear quality (JUNQ) control compartment, whereas the nonubiquitinated, insoluble proteins accumulated in the insoluble protein deposit (IPOD) perivacuolar compartment. Although the overexpressed prion protein Rnq1 was shown to accumulate in the IPOD, the prion status of the cells was not determined. In mammalian cells, misfolded proteins form

Figure 2. Colocalization of [Het-s]ᵧ, [*PSI*⁺], and [*PIN*⁺] dots with cellular compartments. (A) [Het-s]ᵧ internal rings colocalize with the vacuole. Vacuoles of cells with [Het-s]ᵧ rings were stained with FM4-64. Internal [Het-s]ᵧ rings always colocalized with the vacuole. (B) [*PSI*⁺] dots are perivacuolar. [*PSI*⁺] [*PIN*⁺] cells derived from L1749 overexpressing Sup35NM-GFP (from p1066) were stained with DAPI (blue, top) or FM4-64 (red, bottom). [*PSI*⁺] dots were never observed near the nucleus, but were always perivacuolar. (C) Localization of [*PIN*⁺] dots. [*PIN*⁺] cells with single dots (top panels) and multidots (bottom panels) were obtained by overexpressing Rnq1-GFP (from p1415) in low-[*PIN*⁺] (L1943) and high-[*PIN*⁺] (L1749) cells and were stained with DAPI and FM4-64. [*PIN*⁺] single dots are perivacuolar. One of the dots in each multidot [*PIN*⁺] cell is perivacuolar, and one juxtanuclear. (D) [Het-s]ᵧ dots localize to juxtanuclear and perivacuolar compartments. [Het-s]ᵧ dot cultures were stained with either DAPI to stain the nucleus or FM4-64 to stain the vacuolar membrane.
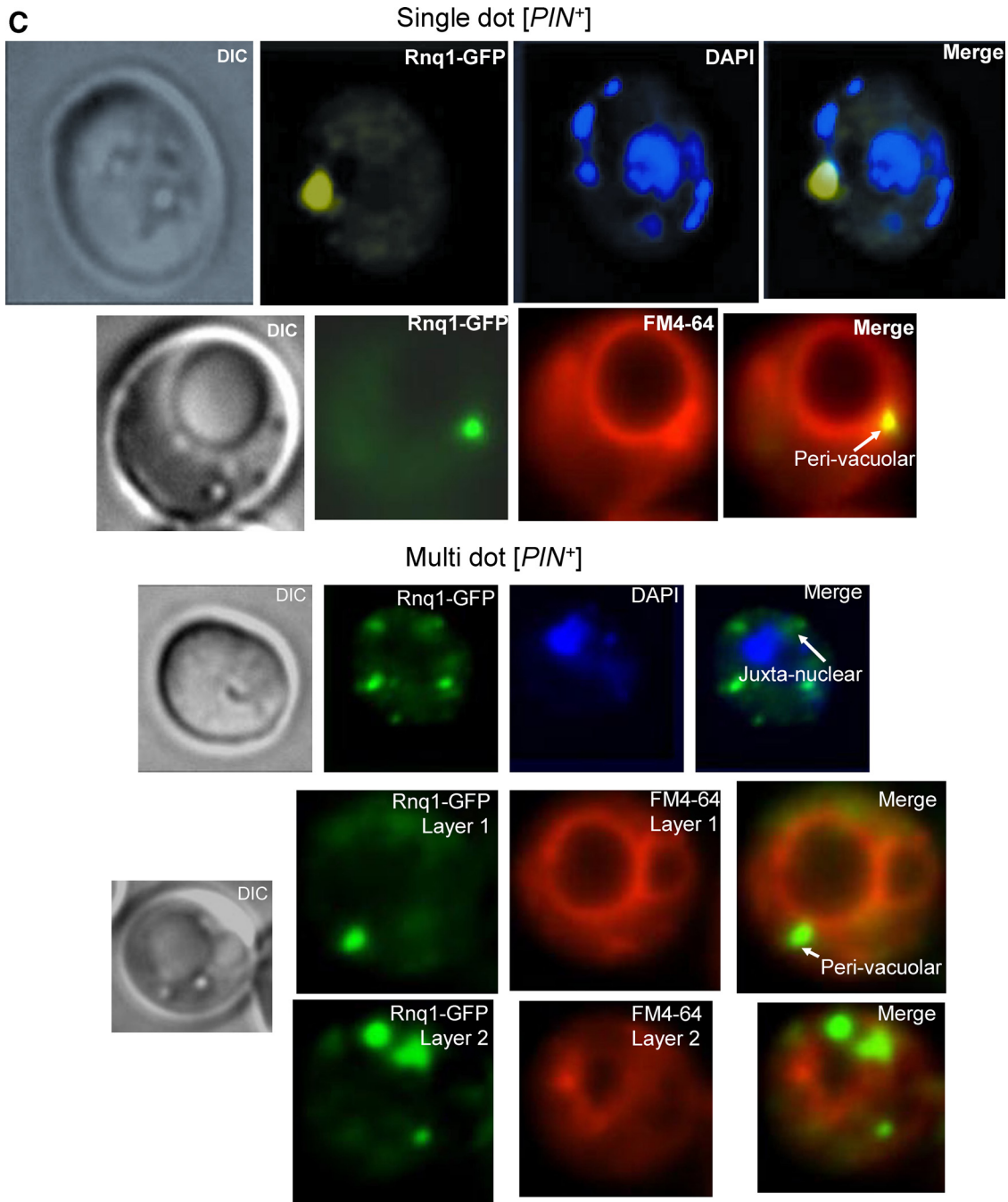
Figure 2. *Continued.*

aggresomes located at the juxtanuclear microtubule organizing center (MTOC; Johnston *et al.,* 1998; Waelter *et al.,* 2001; Shimohata *et al.,* 2002). Also in different yeast studies, polyQ aggregates were shown to localize to the perivacuolar IPOD (Kaganovich *et al.,* 2008) or the juxtanuclear MTOC, the spindle pole body (Wang *et al.,* 2009). Here we asked if, in wild-type prion cells, [*PSI*⁺], [*PIN*⁺] and [Het-s]$_y$ dots localize to perivacuolar and/or juxtanuclear regions.

Cells with single [*PSI*⁺] dots, single- or multi-[*PIN*⁺] dots and two [Het-s]$_y$ dots were obtained and stained with DAPI and FM4-64 to observe the nucleus and the vacuole, respectively. [*PSI*⁺] (Figure 2B) as well as [*PIN*⁺] single dots (Figure 2C, top) were perivacuolar and not juxtanuclear in all of

the 40–50 cells analyzed. Although [*PSI*⁺] aggregates are toxic, about half of the cells with [*PSI*⁺] dots are expected to be alive (Zhou *et al.,* 2001), and [*PSI*⁺] dots were perivacuolar in all the cells analyzed. It is difficult to analyze multidot [*PIN*⁺] because often there are more than two dots, one of which seems to localize near the vacuole and one near the nucleus (Figure 2C, bottom). Whenever multidot [*PIN*⁺] existed as two dots, one dot was perivacuolar and the other juxtanuclear (data not shown). Similarly, one of the two [Het-s]$_y$ dots was always perivacuolar and the other juxtanuclear (Figure 2D). Thus it appears that overexpression of prion protein in the presence of their prions always caused prion proteins to accumulate in a perivacuolar, sometimes
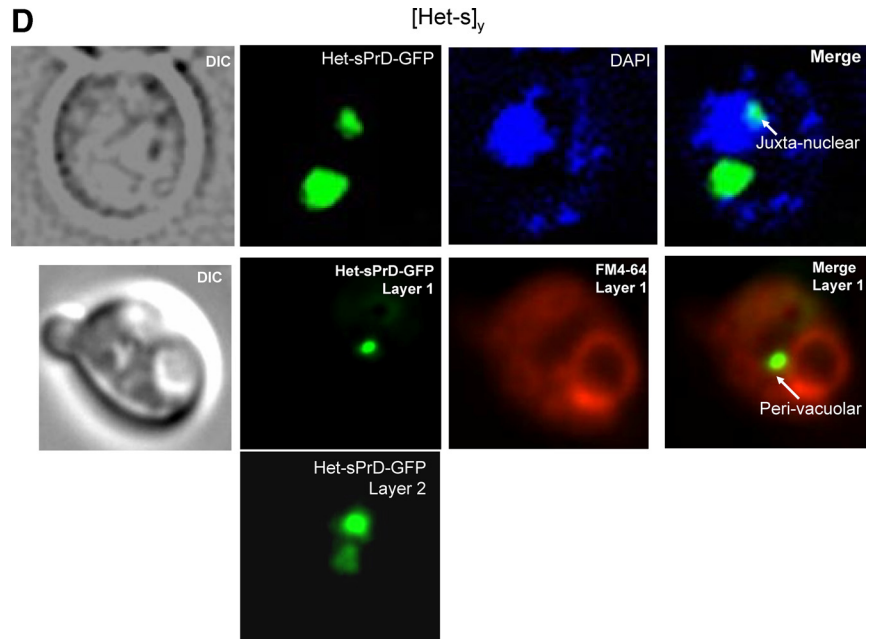
Figure 2. *Continued.*

also in a juxtanuclear compartment, and depending on the variant sometimes also as other cytoplasmic deposits.

Mutations of Genes Involved in Endocytosis Reduce [Het-s]ᵧ Ring Formation, But Endocytosis Is Not Required for [Het-s]ᵧ Propagation

GFP- or cyan fluorescent protein (CFP)-tagged *Het-sPrD* plasmids were transformed into *sla1Δ*, *sla2Δ*, *end3Δ*, and *act1-1* mutants. [Het-s]ᵧ rings were induced in 2% Gal, and the percentage of cells with rings was counted. [Het-s]ᵧ ring formation was completely inhibited in *sla2Δ* cells and was reduced about twofold in *end3Δ* cells, and there was no significant decrease in *sla1Δ* or *act1-1R177A* cells (Figure 3).

Because these proteins are involved in endocytosis, we tested if endocytosis was necessary for the conversion of peripheral rings to internal rings and the subsequent generation of dots, by following cells with peripheral rings that carry the endocytosis mutant, *end3Δ*. [Het-s]ᵧ peripheral rings underwent the same sequence of events in *end3Δ* and isogenic wild-type cells, in at least 15 *end3Δ* ring cells observed. The daughters gave rise to cells with two dots each and the peripheral ring in the mother shrank to form an internal vacuolar ring (Figure 4). Thus, endocytosis is not required for formation of internal rings and dots. The defect in endocytosis in *end3Δ* was confirmed by the lack of uptake of the endocytic dye, Lucifer yellow, in these cells (data not shown).

[PSI⁺] and [Het-s]ᵧ Can Propagate in sla2Δ Cells

Because *sla2Δ* inhibits [*PSI*⁺] and [Het-s]ᵧ formation and was also reported to be lethal in [*PSI*⁺] [*PIN*⁺] cells (Ganusova *et al.*, 2006), we next asked if *sla2Δ* is lethal with [*PSI*⁺] (in [*pin*⁻] cells) and if it is essential for [*PSI*⁺] and [Het-s]ᵧ propagation. [*PSI*⁺] [*pin*⁻] cells (L2285) were mated with *sla2Δ* cells (DDY2740). Selected diploids were sporulated, and [*PSI*⁺] was observed in viable *sla2Δ* spores, although the viability of *sla2Δ* spores was reduced in the [*psi*⁻] pedigree relative to the [*psi*⁻] pedigree (p = 0.1–0.5): 17.5% of the expected *sla2Δ* [*PSI*⁺] spores (20 tetrads dis-

sected) were viable compared with 34.6% of *sla2Δ* [*psi*⁻] spores (13 tetrads dissected). The *sla2Δ* [*PSI*⁺] spores were mated with [*psi*⁻] [*pin*⁻] cells expressing Sup35NM-GFP, and the fused cells or zygotes showed fluorescent foci, indicative of [*PSI*⁺] (Supplementary Figure 4). Semidenaturing agarose gel analysis of cell lysates that detects detergent-resistant amyloid oligomers of prions (Kryndushkin *et al.*, 2003; Bagriantsev *et al.*, 2006) confirmed that *sla2Δ* cells retained [*PSI*⁺] (not shown). In contrast, Ganusova *et al.* (2006) showed that *sla2Δ* is lethal in [*PSI*⁺] [*PIN*⁺] cells in a yeast background derived from strain 74D-694. This appears to be a strain background issue because we also failed to
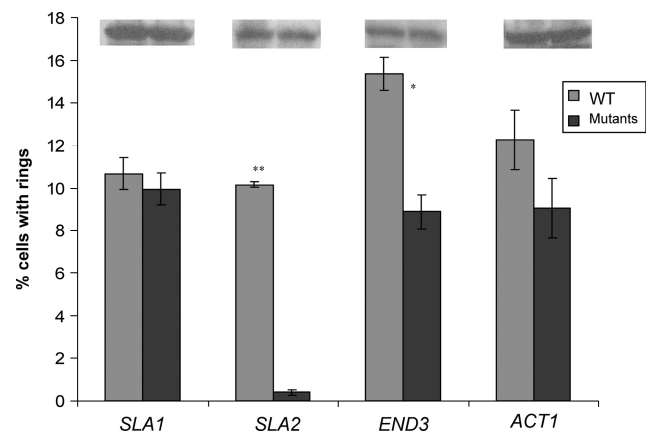

Figure 3. Actin cytoskeletal mutants decrease [Het-s]ᵧ ring formation. [Het-s]ᵧ rings were induced by overexpressing *Het-sPrD-GFP* (p1393) or *Het-sPrD-CFP* (p1470) in *sla1Δ* (GF682), *sla2Δ* (DDY2740), *end3Δ* (GF683), and *act1-1* (L1749 *act1-1R177A*; dark gray) and the isogenic wild types (light gray). The number of cells with rings and diffuse fluorescence were counted after 24 h in 2% Gal. At least 300 cells were counted from each of three independent transformants in each experiment. The averages are shown. Error bars, SE. Statistically significant results, *p = 0.5–0.9; extremely statistically significant, **p > 0.99. Insets, Western blots with no difference in tagged Het-sPrD protein levels in mutant and wild-type cells.
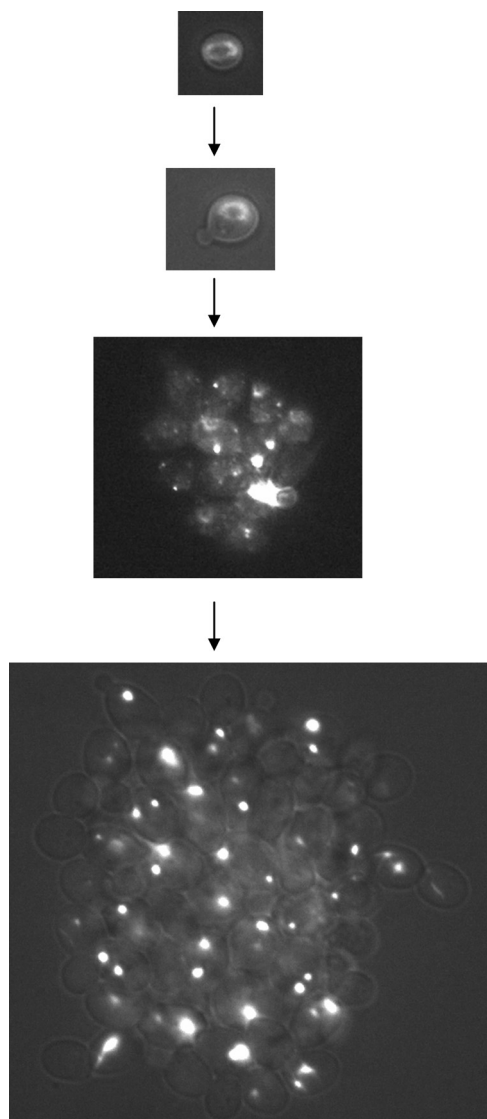
Figure 4. Endocytosis mutant cells with [Het-s]$_y$ rings give rise to cells with [Het-s]$_y$ dots. Het-sPrD-GFP was overexpressed in *end3Δ* to obtain rings, which were micromanipulated and grown on 0.05% Gal medium to follow the appearance of [Het-s]$_y$ aggregates. Similar to isogenic wild type (not shown here), all 15 *end3Δ* [Het-s]$_y$ ring cells examined (one example is shown) gave rise to cells with no fluorescence and then to numerous tiny dots, which finally became two dots. Similar results were seen for another endocytosis mutant, *erg2Δ* (not shown).

Figure 5. Sla2 is not essential for [Het-s]$_y$ propagation. (A) [Het-s]$_y$ dots can propagate in *sla2Δ*. [Het-s]$_y$ dot colonies after loss of *SLA2* plasmid (pDD353) in *sla2Δ* cells (DDY2740) were transferred and grown on 0.05% Gal four times. As a control, the *SLA2* plasmid was retained, transferred, and grown on 0.05% Gal four times. The graph shows percentage of cells with [Het-s]$_y$ dots after each transfer; error bars, ±SE. The *sla2Δ* cells that propagated [Het-s]$_y$ dots, after losing the *SLA2* plasmid, were not extragenic suppressors that restored Sla2 activity, because they still lacked the ability to induce [Het-s]$_y$ rings when the plasmid carrying Het-sPrD-GFP was lost and reintroduced into the same cells (not shown). (B) [Het-s]$_y$ rings (obtained using p1470) were micromanipulated from *sla2Δ* cells expressing *SLA2* under the repressible *Tet0* operator (from p1834) and grown on 0.05% Gal with or without 20 µg/ml doxycycline to repress Sla2 expression. Cells with rings gave rise to cells with dots on control as well as doxycycline plates. Western blots with anti-Sla2N antibody show that Sla2 is not expressed in the presence (+), whereas it is expressed in the absence (−) of 20 µg/ml doxycycline. The expression of Het-sPrD-CFP (detected using cross-reactive anti-GFP antibody) is unaffected.

obtain viable *sla2Δ* [*PSI*⁺] [*pin*⁻] cells in 74D-694 (data not shown). Thus, we show that the absence of [*PSI*⁺] rings in *sla2Δ* cells is not due to toxicity associated with the appearance of [*PSI*⁺].

To test if [Het-s]$_y$ dots could propagate in the absence of Sla2, [Het-s]$_y$ dot containing cells were obtained in *sla2Δ* cells with a plasmid bearing *SLA2* under its own promoter. The *SLA2* plasmid was then lost to check for dot maintenance in the absence of *SLA2* (see *Materials and Methods*). The percentage of cells with [Het-s]$_y$ dots in *SLA2* and *sla2Δ* cultures is shown after growth and three consecutive replica-platings onto 0.05% Gal in Figure 5A. The cells that had lost the *SLA2* plasmid still retained [Het-s]$_y$ dots. Thus, [Het-s]$_y$ can propagate in sla2Δ cells.
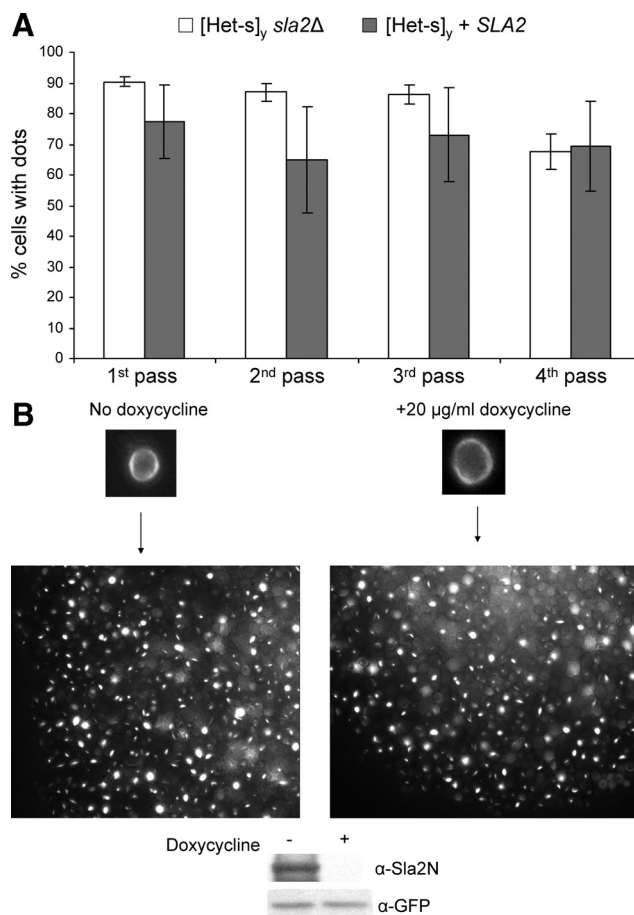
To confirm this result, we constructed a plasmid containing *SLA2* under the control of the repressible *Tet0* box repressor (*Tet0-SLA2*). The *Tet0-SLA2* and *Het-sPrD-CFP* plasmids were transformed into sla2Δ cells, in which [Het-s]$_y$ rings were induced by growth on 2% Gal medium. Single cells with [Het-s]$_y$ rings were micromanipulated and grown on 0.05% Gal media containing 20 µg/ml doxycycline to repress *SLA2* expression. As a control, some cells with rings were grown on media lacking doxycycline. After 5 d, micro-colonies arising from ring cells were observed under the microscope for the presence of [Het-s]$_y$ dots. [Het-s]$_y$ ring cells efficiently gave rise to cells with dots whether colonies

Figure 6. Sla2 interacts with Het-sPrD-GFP. (A) Sla2 interacts with prion and nonprion forms of Het-sPrD-GFP. Plasmids containing Het-sPrD-GFP (p1393) and nonaggregating mutant Het-sPrD (T266P)-GFP (p1525), transformed into [*psi*⁻] [*PIN*⁺] (L1749) cells, were induced in 2% Gal to obtain [Het-s]ᵧ ring and diffuse cultures. Crude cell lysates were made from these cultures and immunoprecipitated with (+) or without (−) anti-GFP antibody for 2 h and incubated with protein G magnetic beads. The beads were then purified and washed on a magnetic column. Specifically bound proteins were eluted at 95°C in SDS-containing buffer and analyzed on a Western blot with anti-Sla2N antibody. Input shows that equal amounts of crude lysates were loaded onto the columns whether anti-GFP antibody was present or not. Eluate shows the proteins that were eluted specifically with Het-sPrD-GFP. For both ring and diffuse cultures, Sla2 is pulled out with Het-sPrD-GFP. Anti-Pgk1 antibody was used as a control to show that there was no nonspecific binding. (B) Sla2Δ33-359, but not Sla2Δ33-359, 576ˢᵗᵒᵖ, interacts with [Het-s]ᵧ. [Het-s]ᵧ rings were induced in *sla2*Δ cells containing Sla2Δ33-359 or Sla2Δ33-359, 576ˢᵗᵒᵖ for 2 d. Crude lysates were used to immunocapture Het-sPrD-CFP with (+) or without (−) cross-reactive anti-GFP antibody. Eluates show proteins that were eluted specifically with Het-sPrD-CFP.
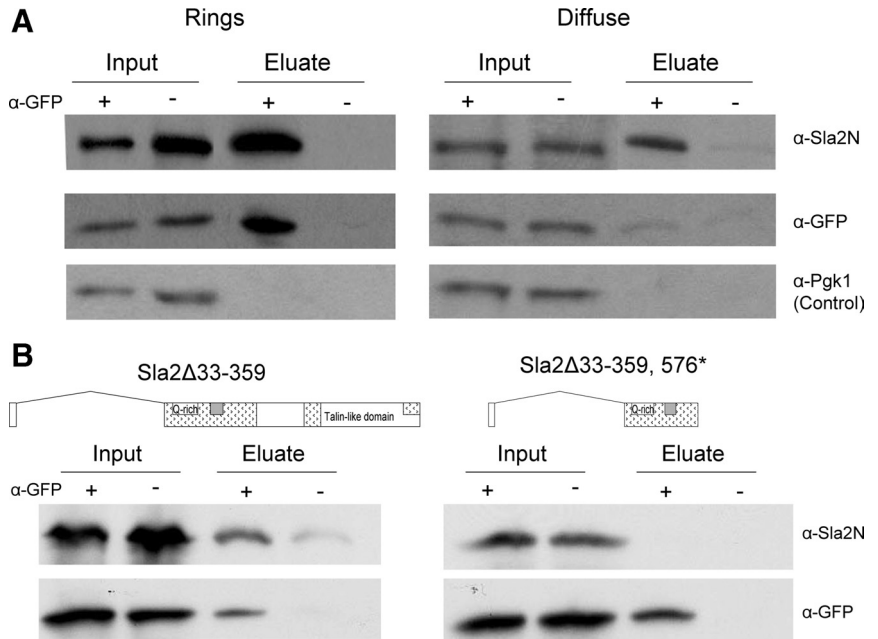
were grown with or without doxycycline (Figure 5B). Although there may be residual Sla2 in the first few daughters, allowing the peripheral ring to collapse into an internal ring and to give rise to daughter cells with dots, these data confirm that [Het-s]ᵧ dots can propagate when Sla2 is diluted out in the later stages of colony growth. The absence of the Sla2 protein was confirmed by Western blot analysis of cell lysates obtained from cells grown with or without doxycycline (Figure 5B).

Sla2 Interacts with [Het-s]ᵧ

Because deletion of *sla2* inhibits [Het-s]ᵧ induction (Figure 3), Sla2 protein may play a role in prion formation by associating with monomers and/or the newly formed prion aggregate. A [Het-s]ᵧ ring culture, formed by overexpressing Het-sPrD-GFP in 2% Gal, and a Het-sPrD-GFP diffuse culture, obtained by overexpressing a point mutant Het-sPrD (T266P)-GFP previously shown to be defective in prion formation (Coustou *et al.*, 1999; Taneja *et al.*, 2007), were used to test if Sla2 is coimmunocaptured with *Het-sPrD-GFP* in the emerging prion and the nonprion forms. Het-sPrD-GFP was immunocaptured with anti-GFP antibody using protein G–labeled magnetic beads. Figure 6A shows that in ring and diffuse cultures, Sla2 was pulled out along with Het-sPrD-GFP, consistent with the idea that Sla2 acts as a scaffold helping to accumulate monomers and stabilize interactions between monomer and emerging prion seeds.

[Het-s]ᵧ Ring Formation Requires Either the Sla2-N Or Q-rich Domain

Mutants deleted in different regions of Sla2 were tested for effects on the induction of [Het-s]ᵧ. Plasmids expressing different fragments of Sla2 (described in Yang *et al.*, 1999) were cotransformed with the *Het-sPrD-CFP* expressing plasmid in a *sla2*Δ background, so that the Sla2 fragment is the only copy of Sla2 expressed. [Het-s]ᵧ was induced to form rings on 2% Gal, and the percentage of cells with rings was determined. All fragments containing the N-terminal ENTH domain that binds to PIP2 and is sufficient for Sla2 function (Wesp *et al.*, 1997; Yang *et al.*, 1999; Sun *et al.*, 2005), namely Sla2Δ360-575, Sla2Δ502-968, Sla2Δ768-968, and full-length Sla2, completely rescued the [Het-s]ᵧ ring formation (Figure 7). In addition, a fragment lacking the N-terminal domain but containing the Q-rich region (Sla2Δ33-359,576ˢᵗᵒᵖ), was also able to rescue [Het-s]ᵧ ring formation. This fragment is not functional, does not localize to the membrane (Yang *et al.*, 1999), and no interaction was detected between it and [Het-s]ᵧ in the coimmunocapture assay (Figure 6B). Surprisingly, a larger fragment (Sla2Δ33-359), which contains the Q-rich domain, localizes to the nonactin cortical patches on the membrane (Yang *et al.*, 1999), and interacts with [Het-s]ᵧ (Figure 6B), is unable to aide [Het-s]ᵧ ring formation.

[Het-s]ᵧ Aggregates Do Not Cause Toxicity

Cells with [*PSI*⁺] rings have a 50–70% reduction in viability compared with cells with diffuse fluorescence (Zhou *et al.*, 2001; Ganusova *et al.*, 2006). To test if [Het-s]ᵧ aggregates cause toxicity, single cells with [Het-s]ᵧ rings and dots were micromanipulated and their growth was examined. Unlike control [*PSI*⁺] cells examined in parallel, there was no significant difference in viability between wild-type cells with or without [Het-s]ᵧ rings (Figure 8) or dots (not shown). Furthermore, cytoskeletal mutants (*sla1*Δ, *end3*Δ, and *act1-1R177A*) did not cause any difference in viability of cells with or without [Het-s]ᵧ rings and dots.

DISCUSSION

Despite the dramatic structural and compositional differences between [*PSI*⁺] and [Het-s]ᵧ, there are several striking similarities: efficient de novo induction of [*PSI*⁺] and [Het-s]ᵧ occurs when Sup35NM-GFP or Het-sPrD-GFP, respectively, are overexpressed, leading to cells with peripheral ring aggregates that later internalize to surround the vacuole. The ring aggregates remain in the mother cell, whereas the daughters propagate the prion as dot-like aggregates. Fur-
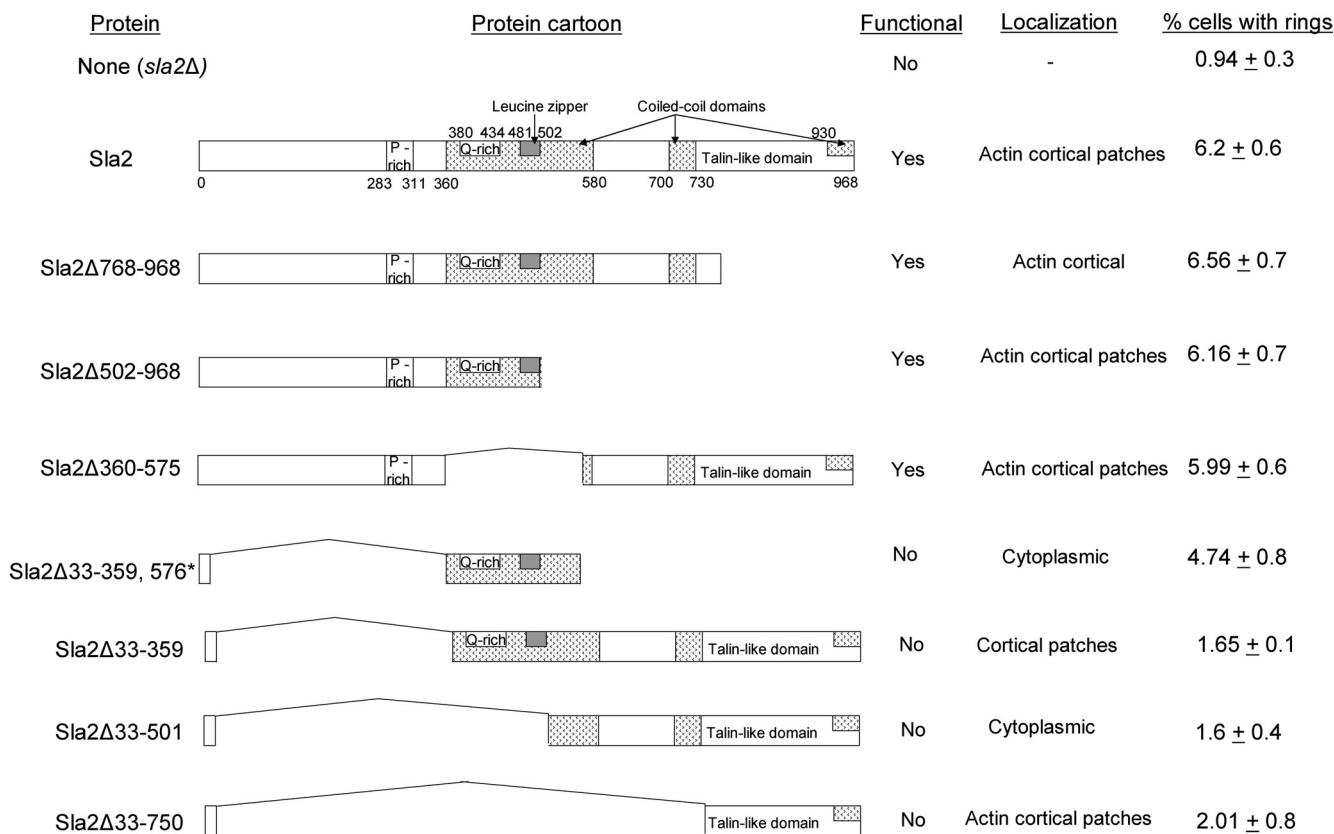
Protein	Protein cartoon	Functional	Localization	% cells with rings
None (*sla2Δ*)		No	-	0.94 ± 0.3
Sla2		Yes	Actin cortical patches	6.2 ± 0.6
Sla2Δ768-968		Yes	Actin cortical	6.56 ± 0.7
Sla2Δ502-968		Yes	Actin cortical patches	6.16 ± 0.7
Sla2Δ360-575		Yes	Actin cortical patches	5.99 ± 0.6
Sla2Δ33-359, 576*		No	Cytoplasmic	4.74 ± 0.8
Sla2Δ33-359		No	Cortical patches	1.65 ± 0.1
Sla2Δ33-501		No	Cytoplasmic	1.6 ± 0.4
Sla2Δ33-750		No	Actin cortical patches	2.01 ± 0.8

Figure 7. Sla2 fragments can rescue [Het-s]$_y$ ring formation in *sla2Δ*. Plasmid containing *Het-sPrD-CFP* (p1470) was either cotransformed with plasmids carrying the different Sla2 truncation fragments (or empty vector) in *sla2Δ* cells (DDY2740) or was transformed into Sla2Δ768-968 and Sla2Δ502-968 yeast strains. [Het-s]$_y$ rings were induced in 2% Gal liquid medium at room temperature, and the percent of cells with rings was determined after 48 h of induction (±SE). The functionality and localization of each fragment in the cell is listed (Yang *et al.,* 1999).

thermore, the cellular locations of these dots are similar for [*PSI*$^+$] and [Het-s]$_y$. Finally, [*PSI*$^+$] and [Het-s]$_y$ require Sla2 for ring formation, but not propagation. These data suggest that different prions require similar cellular machinery for
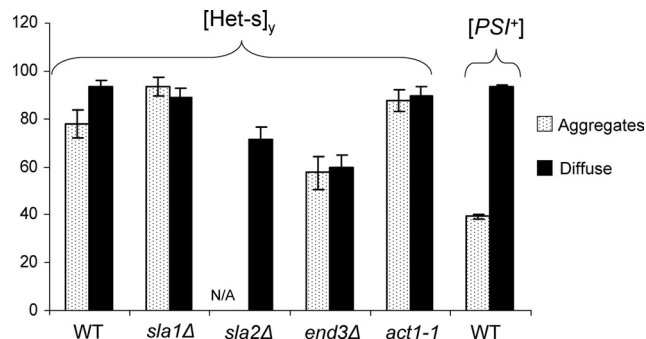

Figure 8. [Het-s]$_y$ rings and dots are not toxic to cells. Individual cells with [Het-s]$_y$ (and [*PSI*$^+$]) rings (aggregates) or diffuse fluorescence (diffuse) in [*psi*$^-$] [*PIN*$^+$] cells (L1749) were micromanipulated in wild-type (WT) or cytoskeletal mutants (*sla1Δ*, *sla2Δ*, *end3Δ*, and *act1-1R177A*) and the ability to form colonies (% viability) was determined. No rings were found in *sla2Δ* cells. All the colonies that arose from ring cells in WT or mutant populations, propagated [Het-s]$_y$ as dots (not shown). Results are averages of three independent experiments, each of which tested at least 20 cells, with and without aggregates, for viability.

their formation and use a similar mode of propagation from cell to cell.

We suggest that the first step in de novo prion induction is the formation of a single prion seed at the cell periphery, followed by a stage in which the seed grows bidirectionally into a peripheral line by the addition of nonprion conformers to both ends of the seed. The aggregate would then continue to grow as a straight line, curving along the cell membrane, resulting in a ring-like mesh that could exceed the diameter of the cell (Figure 1A).

Furthermore, our time-lapse data, for both [*PSI*$^+$] and [Het-s]$_y$, support the hypothesis (Ganusova *et al.,* 2006) that the peripheral ring then internalizes to surround the vacuole. Occasionally it appears that a peripheral line in a mother cell enters the bud and continues along the bud periphery before returning to the mother cell. In addition, some internal rings seem to bridge mother and daughter cells as if they are transferred to the daughter cell along the vacuolar membrane. The appearance of Het-s-GFP aggregates around vacuolar structures has also been observed in *Podospora*, suggesting that the mechanism of prion aggregation is conserved (Coustou-Linares *et al.,* 2001).

Although cells with [*PSI*$^+$] rings and dots are less viable compared with cells with no aggregates (Zhou *et al.,* 2001; Ganusova *et al.,* 2006), we show that cells with or without [Het-s]$_y$ aggregates are equally viable even in the presence of cytoskeletal mutants (Figure 8). Likewise, unlike [*PSI*$^+$] (Dagkesamanskaya and Ter-Avanesyan, 1991; Derkatch *et*

al., 1996), overexpression of Het-sPrD-GFP does not cause toxicity in [Het-s]$_y$ cells (data not shown). This is not surprising because Het-sPrD-GFP is not an essential yeast protein, and [*PSI*+] toxicity due to the overexpression of the Sup35 prion domain was recently shown to be due to sequestration of the essential Sup35 into [*PSI*+] aggregates, thereby depleting Sup35 from the cell (Vishveshwara *et al.*, 2009).

It has been suggested that protein aggregates in inclusion bodies are seeded at a single or limited number of nucleation sites (Kopito, 2000). Furthermore, [*PSI*+] prion and polyQ aggregates have been hypothesized to assemble at endocytic sites because several components of the endocytic site (Sla1, Sla2, and Act1) interact with Sup35 and enhance, or are required for, [*PSI*+] induction (Ganusova *et al.*, 2006) and polyQ aggregation (Meriin *et al.*, 2007). Also, in agreement with this hypothesis, Hip1, the mammalian homolog of Sla2, interacts with the polyQ Huntingtin protein (Kalchman *et al.*, 1997). Our current finding that Sla2 is required for [Het-s]$_y$ formation but not for [*PSI*+] and [Het-s]$_y$ propagation (Figures 3 and 5, A and B) and that Sla2 physically interacts with monomeric and aggregated Het-sPrD-GFP (Figure 6A) further supports this hypothesis. Thus, prion monomers, concentrated at the membrane, would be poised to propagate any conformational change to the prion form. In addition, our data for [Het-s]$_y$ (Figure 4) indicate that once the prion ring appears, endocytosis is not required for internal ring formation or prion dot propagation. Also, our finding that [*PSI*+] and [Het-s]$_y$ aggregates can propagate in *sla2Δ* shows that Sla2's major role is during prion ring formation.

Findings here and elsewhere (Ganusova *et al.*, 2006) that the actin cortical cytoskeletal protein, Sla2, is essential for prion induction and binds prion proteins led to the hypothesis that Sla2 is required to attract and tether overexpressed prion proteins, thereby aiding the formation of a prion seed. This hypothesis also explained why de novo prion aggregates first appear at the membrane. However, other findings in our current work now challenge this hypothesis. Indeed, replacing Sla2 with the Sla2Δ33-359, 576^{stop} fragment that is not located at the membrane and fails to bind Het-sPrD-GFP still permits [Het-s]$_y$ ring and prion formation (Figures 6B and 7). Possibly the Q-rich stretch retained in Sla2Δ33-359, 576^{stop} interacts transiently with prion protein to promote seed formation. However, a deletion lacking this Q-rich stretch (Sla2Δ360-575) but sufficient for Sla2 function (Wesp *et al.*, 1997; Yang *et al.*, 1999) was also sufficient for efficient [Het-s]$_y$ prion ring formation (Figure 7). It could be that prion formation requires either the seeding activity of the Q-rich segment of Sla2 *or* Sla2's ability to bring prion proteins to the actin patches on the membrane. However, one fragment (Sla2Δ33-359) that retained the Q-rich segment, which localized to the nonactin cortical patches and which bound [Het-s]$_y$ (Figure 6B), still did not support [Het-s]$_y$ ring formation (Figure 7), suggesting that just the interaction of Sla2 and [Het-s]$_y$ is not sufficient for ring formation. Possibly the altered conformation in this larger fragment interferes with prion seed formation by negatively regulating the Q-rich function. We suggest that de novo prion formation requires either, but not both, the Sla2-N or Q-rich domains. Because either of these domains is independently dispensable for prion formation, it appears that other proteins can also provide these activities.

When Sup35-GFP is expressed at endogenous levels [*PSI*+] exists and propagates as numerous, tiny dots (Satpute-Krishnan and Serio, 2005). Similarly, we initially observed the appearance of numerous, tiny dots in [Het-s]$_y$ daughters in [*pin*−] cells (Figure 1C). Later, for [Het-s]$_y$,

these numerous dots became three or four larger dots and finally just two dots. Likewise, overexpression of prion proteins in the homologous prion-containing cell is known to cause larger aggregates to appear: when Sup35-GFP is overexpressed in [*PSI*+] cells, one big [*PSI*+] dot is seen (Patino *et al.*, 1996; Zhou *et al.*, 2001); overexpressed GFP-tagged Rnq1 or Ure2 in the presence of [*PIN*+] and [URE3], respectively, causes the appearance of bigger foci (Edskes *et al.*, 1999; Bradley and Liebman, 2003; Crapeau *et al.*, 2009); Het-s-GFP aggregation into dots in [Het-s] strains in *Podospora* only occurs when Het-s-GFP is overexpressed under a strong promoter (Coustou-Linares *et al.*, 2001). The two big fluorescent dots seen in [Het-s]$_y$ cells seem similar to these concentration-dependent larger aggregates (Figure 1, C and D). It is important to recall that these bigger foci are not the transmissible prion seeds, because they almost always remained in the mother cell. Thus, the line, ring, mesh, and dot aggregates should only be regarded as phenotypic markers of the presence of the infectious prion seeds. This mechanism of keeping large aggregates in the mother may be used to prevent damaged proteins from being passed on to daughters.

In [*PIN*+] cells, the process of [Het-s]$_y$ dot formation seems to be accelerated, and we could not observe the numerous dot stage (Figure 1D). Because [*PIN*+] is known to enhance the de novo formation of heterologous prions (Derkatch *et al.*, 2001; Taneja *et al.*, 2007; Mathur *et al.*, 2009), it is not surprising that [*PIN*+] enhanced [Het-s]$_y$ aggregation.

We tested if the big dots are protein deposits localizing to perivacuolar or juxtanuclear compartments. Kaganovich *et al.* (2008) found that misfolded proteins, in yeast proteasomal mutants, deposit in the perivacuolar (IPOD) and the juxtanuclear (JUNQ) compartments. The amyloid-forming insoluble proteins (overexpressed Rnq1 and polyQ) were deposited only at the perivacuolar IPOD (Kaganovich *et al.*, 2008). In another study, polyQ aggregates instead colocalized with the yeast spindle pole body (Wang *et al.*, 2009), which is analogous to the mammalian juxtanuclear MTOC, where misfolded protein aggregates are deposited (Johnston *et al.*, 1998; Waelter *et al.*, 2001; Shimohata *et al.*, 2002). We found that [*PSI*+] and [*PIN*+] single dots localized to a perivacuolar compartment (Figure 2, B and C; suggestive of IPOD). In the case of multidots (as in [Het-s]$_y$ and [*PIN*+]), one of the dots in all cells was also perivacuolar, and another dot was always juxtanuclear (Figure 2, C and D). The juxtanuclear aggregates we see may be equivalent to JUNQ or the spindle pole body.

The appearance of prion aggregates has been related to mammalian aggresomes, and it has been suggested that the aggregation of QN-rich, insoluble proteins occurs because of the inability of the proteasomal machinery to degrade the excess protein (Ganusova *et al.*, 2006). Likewise, it has been suggested that protein oligomers in mammalian cells assemble at the cell surface and then move inward to deposit as aggresomes (Kopito, 2000). Our data showing that prion monomers first assemble into ring/mesh-like aggregates at the cell surface and later move inward to deposit at one of the cellular compartments are consistent with the hypothesis suggested for aggresome formation. However, the correlation between mammalian aggresomes and the yeast JUNQ, IPOD, and spindle pole body remains to be established.

REFERENCES

Alberti, S., Halfmann, R., King, O., Kapila, A., and Lindquist, S. (2009). A systematic survey identifies prions and illuminates sequence features of prionogenic proteins. Cell *137*, 146–158.

Bagriantsev, S. N., Gracheva, E. O., Richmond, J. E., and Liebman, S. W. (2008). Variant-specific [PSI+] infection is transmitted by Sup35 polymers within [PSI+] aggregates with heterogeneous protein composition. Mol. Biol. Cell *19*, 2433–2443.

Bagriantsev, S. N., Kushnirov, V. V., and Liebman, S. W. (2006). Analysis of amyloid aggregates using agarose gel electrophoresis. Methods Enzymol. *412*, 33–48.

Bailleul, P. A., Newnam, G. P., Steenbergen, J. N., and Chernoff, Y. O. (1999). Genetic study of interactions between the cytoskeletal assembly protein sla1 and prion-forming domain of the release factor Sup35 (eRF3) in *Saccharomyces cerevisiae.* Genetics *153*, 81–94.

Balguerie, A. *et al.* (2003). Domain organization and structure-function relationship of the HET-s prion protein of *Podospora anserina.* EMBO J. *22*, 2071–2081.

Baxa, U., Wickner, R. B., Steven, A. C., Anderson, D. E., Marekov, L. N., Yau, W. M., and Tycko, R. (2007). Characterization of beta-sheet structure in Ure2p1–89 yeast prion fibrils by solid-state nuclear magnetic resonance. Biochemistry *46*, 13149–13162.

Brachmann, A., Baxa, U., and Wickner, R. B. (2005). Prion generation in vitro: amyloid of Ure2p is infectious. EMBO J. *24*, 3082–3092.

Bradley, M. E., Edskes, H. K., Hong, J. Y., Wickner, R. B., and Liebman, S. W. (2002). Interactions among prions and prion "strains" in yeast. Proc. Natl. Acad. Sci. USA *99*(Suppl 4), 16392–16399.

Bradley, M. E., and Liebman, S. W. (2003). Destabilizing interactions among [PSI(+)] and [PIN(+)] yeast prion variants. Genetics *165*, 1675–1685.

Coustou-Linares, V., Maddelein, M. L., Begueret, J., and Saupe, S. J. (2001). In vivo aggregation of the HET-s prion protein of the fungus *Podospora anserina.* Mol. Microbiol. *42*, 1325–1335.

Coustou, V., Deleu, C., Saupe, S., and Begueret, J. (1997). The protein product of the het-s heterokaryon incompatibility gene of the fungus *Podospora anserina* behaves as a prion analog. Proc. Natl. Acad. Sci. USA *94*, 9773–9778.

Coustou, V., Deleu, C., Saupe, S. J., and Begueret, J. (1999). Mutational analysis of the [Het-s] prion analog of *Podospora anserina*. A short N-terminal peptide allows prion propagation. Genetics *153*, 1629–1640.

Crapeau, M., Marchal, C., Cullin, C., and Maillet, L. (2009). The cellular concentration of the yeast Ure2p prion protein affects its propagation as a prion. Mol. Biol. Cell *20*, 2286–2296.

Dagkesamanskaya, A. R., and Ter-Avanesyan, M. D. (1991). Interaction of the yeast omnipotent suppressors SUP1(SUP45) and SUP2(SUP35) with non-mendelian factors. Genetics *128*, 513–520.

DePace, A. H., Santoso, A., Hillner, P., and Weissman, J. S. (1998). A critical role for amino-terminal glutamine/asparagine repeats in the formation and propagation of a yeast prion. Cell *93*, 1241–1252.

Derkatch, I. L., Bradley, M. E., Hong, J. Y., and Liebman, S. W. (2001). Prions affect the appearance of other prions: the story of [PIN(+)]. Cell *106*, 171–182.

Derkatch, I. L., Bradley, M. E., Masse, S. V., Zadorsky, S. P., Polozkov, G. V., Inge-Vechtomov, S. G., and Liebman, S. W. (2000). Dependence and independence of [PSI(+)] and [PIN(+)]: a two-prion system in yeast? EMBO J. *19*, 1942–1952.

Derkatch, I. L., Bradley, M. E., Zhou, P., Chernoff, Y. O., and Liebman, S. W. (1997). Genetic and environmental factors affecting the de novo appearance of the [PSI+] prion in *Saccharomyces cerevisiae.* Genetics *147*, 507–519.

Derkatch, I. L., Chernoff, Y. O., Kushnirov, V. V., Inge-Vechtomov, S. G., and Liebman, S. W. (1996). Genesis and variability of [PSI] prion factors in *Saccharomyces cerevisiae.* Genetics *144*, 1375–1386.

Du, Z., Park, K. W., Yu, H., Fan, Q., and Li, L. (2008). Newly identified prion linked to the chromatin-remodeling factor Swi1 in *Saccharomyces cerevisiae.* Nat. Genet. *40*, 460–465.

Edskes, H. K., Gray, V. T., and Wickner, R. B. (1999). The [URE3] prion is an aggregated form of Ure2p that can be cured by overexpression of Ure2p fragments. Proc. Natl. Acad. Sci. USA *96*, 1498–1503.

Ganusova, E. E., Ozolins, L. N., Bhagat, S., Newnam, G. P., Wegrzyn, R. D., Sherman, M. Y., and Chernoff, Y. O. (2006). Modulation of prion formation,

aggregation, and toxicity by the actin cytoskeleton in yeast. Mol. Cell. Biol. *26*, 617–629.

Gari, E., Piedrafita, L., Aldea, M., and Herrero, E. (1997). A set of vectors with a tetracycline-regulatable promoter system for modulated gene expression in *Saccharomyces cerevisiae.* Yeast *13*, 837–848.

Gietz, R. D., and Woods, R. A. (2002). Transformation of yeast by lithium acetate/single-stranded carrier DNA/polyethylene glycol method. Methods Enzymol. *350*, 87–96.

Glover, J. R., Kowal, A. S., Schirmer, E. C., Patino, M. M., Liu, J. J., and Lindquist, S. (1997). Self-seeded fibers formed by Sup35, the protein determinant of [PSI+], a heritable prion-like factor of *S. cerevisiae.* Cell *89*, 811–819.

Johnston, J. A., Ward, C. L., and Kopito, R. R. (1998). Aggresomes: a cellular response to misfolded proteins. J. Cell Biol. *143*, 1883–1898.

Kaganovich, D., Kopito, R., and Frydman, J. (2008). Misfolded proteins partition between two distinct quality control compartments. Nature *454*, 1088–1095.

Kalchman, M. A. *et al.* (1997). HIP1, a human homologue of *S. cerevisiae* Sla2p, interacts with membrane-associated huntingtin in the brain. Nat. Genet. *16*, 44–53.

King, C. Y., Tittmann, P., Gross, H., Gebert, R., Aebi, M., and Wuthrich, K. (1997). Prion-inducing domain 2–114 of yeast Sup35 protein transforms in vitro into amyloid-like filaments. Proc. Natl. Acad. Sci. USA *94*, 6618–6622.

Kishimoto, A., Hasegawa, K., Suzuki, H., Taguchi, H., Namba, K., and Yoshida, M. (2004). beta-Helix is a likely core structure of yeast prion Sup35 amyloid fibers. Biochem. Biophys. Res. Commun. *315*, 739–745.

Kopito, R. R. (2000). Aggresomes, inclusion bodies and protein aggregation. Trends Cell Biol. *10*, 524–530.

Krishnan, R., and Lindquist, S. L. (2005). Structural insights into a yeast prion illuminate nucleation and strain diversity. Nature *435*, 765–772.

Kryndushkin, D. S., Alexandrov, I. M., Ter-Avanesyan, M. D., and Kushnirov, V. V. (2003). Yeast [PSI+] prion aggregates are formed by small Sup35 polymers fragmented by Hsp104. J. Biol. Chem. *278*, 49636–49643.

Mathur, V., Hong, J. Y., and Liebman, S. W. (2009). Ssa1 overexpression and [PIN(+)] variants cure [PSI(+)] by dilution of aggregates. J. Mol. Biol. *390*, 155–167.

Meriin, A. B., Zhang, X., Alexandrov, I. M., Salnikova, A. B., Ter-Avanesian, M. D., Chernoff, Y. O., and Sherman, M. Y. (2007). Endocytosis machinery is involved in aggregation of proteins with expanded polyglutamine domains. FASEB J. *21*, 1915–1925.

Nelson, R., Sawaya, M. R., Balbirnie, M., Madsen, A. O., Riekel, C., Grothe, R., and Eisenberg, D. (2005). Structure of the cross-beta spine of amyloid-like fibrils. Nature *435*, 773–778.

Nemecek, J., Nakayashiki, T., and Wickner, R. B. (2009). A prion of yeast metacaspase homolog (Mca1p) detected by a genetic screen. Proc. Natl. Acad. Sci. USA *106*, 1892–1896.

Osherovich, L. Z., Cox, B. S., Tuite, M. F., and Weissman, J. S. (2004). Dissection and design of yeast prions. PLoS Biol. *2*, E86.

Pan, K.-M. *et al.* (1993). Conversion of alpha-helices into beta-sheets features in the formation of the scrapie prion proteins. Proc. Natl. Acad. Sci. USA *90*, 10962–10966.

Patel, B. K., Gavin-Smyth, J., and Liebman, S. W. (2009). The yeast global transcriptional co-repressor protein Cyc8 can propagate as a prion. Nat. Cell Biol. *11*, 344–349.

Patel, B. K., and Liebman, S. W. (2007). "Prion-proof" for [PIN+]: infection with in vitro-made amyloid aggregates of Rnq1p-(132–405) induces [PIN+]. J. Mol. Biol. *365*, 773–782.

Patino, M. M., Liu, J. J., Glover, J. R., and Lindquist, S. (1996). Support for the prion hypothesis for inheritance of a phenotypic trait in yeast. Science *273*, 622–626.

Prusiner, S. B. (1998). Prions. Proc. Natl. Acad. Sci. USA *95*, 13363–13383.

Ritter, C., Maddelein, M. L., Siemer, A. B., Luhrs, T., Ernst, M., Meier, B. H., Saupe, S. J., and Riek, R. (2005). Correlation of structural elements and infectivity of the HET-s prion. Nature *435*, 844–848.

Ross, E. D., M. A., and Wickner, R. B. (2005). Prion domains: sequences, structures and interactions. Nat. Cell Biol. *7*, 1039–1044.

Satpute-Krishnan, P., and Serio, T. R. (2005). Prion protein remodelling confers an immediate phenotypic switch. Nature *437*, 262–265.

Sen, A., B. U., Simon, M. N., Wall, J. S., Sabate, R., Saupe, S. J., and Steven, A. C. (2007). Mass analysis by scanning transmission electron microscopy and electron diffraction validate predictions of stacked beta-solenoid model of HET-s prion fibrils. J. Biol. Chem. *282*, 5545–5550.

Serio, T. R., Cashikar, A. G., Kowal, A. S., Sawicki, G. J., Moslehi, J. J., Serpell, L., Amsdorf, M. F., and Lindquist, S. L. (2000). Nucleated conformational conversion and the replication of conformational information by a prion determinant. Science *289*, 1317–1321.

Sherman, F., Fink, G. R., and Hicks, J. B. (1986). *Methods in Yeast Genetics*, Plainview, NY: Cold Spring Harbor Laboratory Press.

Shewmaker, F., Kryndushkin, D., Chen, B., Tycko, R., and Wickner, R. B. (2009). Two prion variants of Sup35p have in-register parallel ss-sheet structures, independent of hydration. Biochemistry *48*, 5074–5082.

Shewmaker, F., Ross, E. D., Tycko, R., and Wickner, R. B. (2008). Amyloids of shuffled prion domains that form prions have a parallel in-register beta-sheet structure. Biochemistry *47*, 4000–4007.

Shewmaker, F., Wickner, R. B., and Tycko, R. (2006). Amyloid of the prion domain of Sup35p has an in-register parallel beta-sheet structure. Proc. Natl. Acad. Sci. USA *103*, 19754–19759.

Shimohata, T., Sato, A., Burke, J. R., Strittmatter, W. J., Tsuji, S., and Onodera, O. (2002). Expanded polyglutamine stretches form an 'aggresome.' Neurosci. Lett. *323*, 215–218.

Sondheimer, N., and Lindquist, S. (2000). Rnq1, an epigenetic modifier of protein function in yeast. Mol. Cell *5*, 163–172.

Sun, Y., Kaksonen, M., Madden, D. T., Schekman, R., and Drubin, D. G. (2005). Interaction of Sla2p's ANTH domain with PtdIns(4,5)P2 is important for actin-dependent endocytic internalization. Mol. Biol. Cell *16*, 717–730.

Taneja, V., Maddelein, M. L., Talarek, N., Saupe, S. J., and Liebman, S. W. (2007). A non-Q/N-rich prion domain of a foreign prion, [Het-s], can propagate as a prion in yeast. Mol. Cell *27*, 67–77.

Vida, T., and Emr, S. (1995). A new vital stain for visualizing vacuolar membrane dynamics and endocytosis in yeast. J. Cell Biol. *128*, 779–792.

Vishveshwara, N., Bradley, M. E., and Liebman, S. W. (2009). Sequestration of essential proteins causes prion associated toxicity in yeast. Mol. Microbiol. *73*, 1101–1114.

Waelter, S., Boeddrich, A., Lurz, R., Scherzinger, E., Lueder, G., Lehrach, H., and Wanker, E. E. (2001). Accumulation of mutant huntingtin fragments in aggresome-like inclusion bodies as a result of insufficient protein degradation. Mol. Biol. Cell *12*, 1393–1407.

Wang, Y., Meriin, A. B., Zaarur, N., Romanova, N. V., Chernoff, Y. O., Costello, C. E., and Sherman, M. Y. (2009). Abnormal proteins can form aggresome in yeast: aggresome-targeting signals and components of the machinery. FASEB J. *23*, 451–463.

Wasmer, C., Lange, A., Van Melckebeke, H., Siemer, A. B., Riek, R., and Meier, B. H. (2008). Amyloid fibrils of the HET-s(218–289) prion form a beta solenoid with a triangular hydrophobic core. Science *319*, 1523–1526.

Wesp, A., Hicke, L., Palecek, J., Lombardi, R., Aust, T., Munn, A. L., and Riezman, H. (1997). End4p/Sla2p interacts with actin-associated proteins for endocytosis in *Saccharomyces cerevisiae*. Mol. Biol. Cell *8*, 2291–2306.

Wickner, R. B. (1994). [URE3] as an altered URE2 protein: evidence for a prion analog in *Saccharomyces cerevisiae*. Science *264*, 566–569.

Wickner, R. B., Dyda, F., and Tycko, R. (2008a). Amyloid of Rnq1p, the basis of the [PIN+] prion, has a parallel in-register beta-sheet structure. Proc. Natl. Acad. Sci. USA *105*, 2403–2408.

Wickner, R. B., Masison, D. C., and Edskes, H. K. (1995). [PSI] and [URE3] as yeast prions. Yeast *11*, 1671–1685.

Wickner, R. B., Shewmaker, F., Kryndushkin, D., and Edskes, H. K. (2008b). Protein inheritance (prions) based on parallel in-register beta-sheet amyloid structures. Bioessays *30*, 955–964.

Yang, S., Cope, M. J., and Drubin, D. G. (1999). Sla2p is associated with the yeast cortical actin cytoskeleton via redundant localization signals. Mol. Biol. Cell *10*, 2265–2283.

Zhou, P., Derkatch, I. L., and Liebman, S. W. (2001). The relationship between visible intracellular aggregates that appear after overexpression of Sup35 and the yeast prion-like elements [PSI(+)] and [PIN(+)]. Mol. Microbiol. *39*, 37–46.